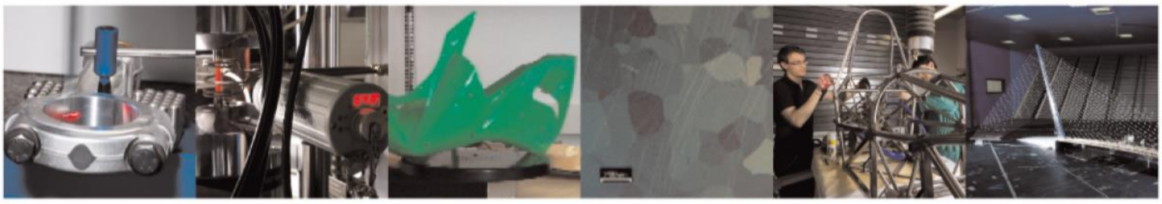

Development of a generalized chatter detection methodology for variable speed machining

Albertelli, Paolo; Braghieri, Luca; Torta, Mattia; Monno, Michele

This is a post-peer-review, pre-copyedit version of an article published in MECHANICAL SYSTEMS AND SIGNAL PROCESSING. The final authenticated version is available online at: http://dx.doi.org/10.1016/j.ymssp.2019.01.002

Development of a generalized chatter detection methodology for variable speed machining

Paolo Albertelli[a,*], Luca Braghieri[b], Mattia Torta[b], Michele Monno[a]

[a]*Department of Mechanical Engineering, Politecnico di Milano, via La Masa 1, 20156 Milan, Italy*

[b]*MUSP Macchine Utensili Sistemi di Produzione, strada della Torre della Razza, 29122 Piacenza, Italy*

Abstract

Regenerative chatter is one of the most deleterious phenomena affecting machining operations. It affects the integrity of the tool and the achievement of the targeted performance both for what concerns the the material removal rate MRR and the quality of the processed surfaces. The majority of the chatter detection algorithms found in literature were not conceived for machining operations performed in non-stationary conditions although, it was demonstrated, that a continuous modulation of the spindle speed (spindle speed variation SSV) is one of the most profitable chatter suppression methodologies. This limitation represents an obstacle to the development of chatter controller systems that need to rely on effective and robust chatter monitoring procedures.

In the present research, a chatter detection algorithm, specifically suitable for dealing with variable speed machining, was thus developed. More in details, the cutting stability assessment, performed in the spindle angular domain, is carried out through the real-time computation of a normalized chatter indicator that refers to the cyclostationary theory. Before computing the chatter indicator, the order tracking and the synchronous averaging methodologies are adopted for pre-processing the vibrational signals and the data coming from the spindle encoder.

The devised chatter monitoring methodology was successfully validated executing real milling operations in which both constant and variable speed

*Corresponding author

Email address: paolo.albertelli@polimi.it (Paolo Albertelli)

machining (SSV) were carried out. It was observed that the developed algorithm is capable of fast and robustly detecting chatter in all the tested cutting conditions.

Keywords:
chatter detection, milling, variable speed machining, SSV, order tracking, cyclostationarity

---

1. Introduction

Regenerative chatter [1] negatively affects the quality of the machined work-pieces, the tool integrity and limits the maximum achievable material removal rate MRR. For these reasons, it still represents a challenge both for manufacturing industries and for the scientific community, Munoa et al. in [2].

According to the scientific literature [3], the suppression of chatter vibrations can even be accomplished by continuously modulating the spindle speed. This approach is typically known as the continuous spindle speed variation SSV. Different modulating strategies (sinusoidal, triangular, random, etc.) were studied over the years. The most analyzed SSV technique was undoubtedly the sinusoidal spindle speed variation $SSSV$, Munoa et al. [2] and Totis et al. [4]).

Despite several studies were carried out on the presented chatter suppression techniques (based on SSV), their real-time implementation on industrial-oriented vibration controllers has not yet successfully reached a satisfactory maturation, [5] and [6]. The main observed limitations are related to the difficulty of adapting the main parameters of the conceived strategies to what really happens during cutting. Another relevant limitation is related to the capability of rapidly perceiving the chatter vibration occurrence and to continuously assess the stability during the implementation of the chatter suppression techniques. For what concerns the detection of chatter, several methodologies were developed and tested over the years but a better comprehension of the limitations of the existing approaches is extremely useful.

Ismail and Kubica in [7] defined a chatter indicator based on the ratio between the dynamic and the static contributions of the cutting forces. It was suitable to be implemented in combination with a chatter suppression controller [6] based on SSV although it was observed that, due to its simplicity, was not sufficiently robust. Moreover, since the indicator was based on force measurements, it was not particularly indicated for real industrial applications. Many studies were focused on the selection of the most suitable signals for monitoring regenerative chatter vibrations. Most of them, as reported in the review of Cao et al. [8], are connected to the spindle system since it is the machine tool component that is mostly affected by vibrations. Some of these researches investigated the potentialities of audio signals, Schmitz ([9] - [10]), Tsai et al. [11] and Quintana et al. in [12]. Aslan and Altintas in [13] developed a chatter detection methodology that exploited the spindle drive current command. Although the proposed methodology for extending the measuring bandwidth seemed working, the efficacy in the chatter detection was far from the one achievable using audio signals. Kuljanic et al. [14] compared some chatter indicators using several different signals (cutting forces, spindle torque, acceleration, etc.) or combinations of them and performed considerations in terms of efficacy and robustness.

Since the chatter related dynamics are characterized by a set of specific frequencies (Insperger et al. [15]), a spectral analysis can be used to detect the occurrence of the instability. Tansel et al. in [16] used a fast Fourier transform FFT to extract amplitudes and frequencies of the main spectral cutting force components. The authors exploited the extracted parameters to feed a index based reasoner IBR that performed the chatter assessment. All the FFT-based algorithms suffer non stationary conditions that typically occur in vibrational controller systems. In order to limit these drawbacks, the short-time Fourier transform ($STFT$) can be used. For instance, Koike et al. in [17] developed a chatter monitoring system that exploits a disturbance observer for real-time estimating the spindle torque that was further analyzed using the $STFT$. An enhanced time-frequency methodology (synchrosqueezing transform (ST)) was used for chatter detection purposes by Cao et al.in [18] and in [19]. Although the $STFT$ is one of the most used spectral-based methodologies for chatter monitoring, a proper balance between time and frequency resolution can not be easily found.

Wavelet-based techniques represent an enhanced extension of other time-frequency distributions. They are particularly suitable for monitoring non stationary processes and therefore they can be used for detecting the onset of chatter vibrations, [20], [21] and [22]. These techniques are adaptable to on-line implementations but their limitations can be critically analyzed.

Choi and Shin in [23] developed a chatter algorithm that was based on the likeness of cutting process related signals to nearly $1/TPF$ signals. The algorithm was successfully tested both in turning and milling but the threshold definition has to be defined accordingly with the specific application. Wang and Liang in [21] developed a normalized statistical chatter index based on the maxima of the modulus of the wavelet transform ($WTMM$). The authors conceived a methodology for automatically defining the chatter threshold. In some cases, the wavelet-based techniques are used in combination to other approaches, Zhang et al. [24].

Unfortunately, for the wavelet based methodologies, there are no theoretical approaches for selecting the best basis. The methodologies require the involvement of advanced skills and consequently they do not fit with the needs of an automatic implementation. These drawbacks are partially reduced using the Hilbert-Huang transform, a time-frequency approach that requires less manual intervention for the signal processing and the signal decomposition (Huang et al. [25]). Most of these researches ([26], [27], [28], [29], [30] and [31]) decomposed the vibrational signals using the ensemble empirical mode decomposition $EEMD$ and selected the the intrinsic mode function $IMFs$ using a defined criterion. A specific normalized chatter indicator was further computed. Although the methodology seems compatible with the on-line implementation, the procedure still requires the selection and/or the tuning of several parameters.

Other approaches, suitable for unstationary and nonlinear phenomena and that do not require the selection of basis functions were investigated by Perez-Canales et al. in [32] and Vela-Martinez et al. in [33] and [34]. Entropy randomness, Hurst exponent and detrended fluctuation analysis DFA are some of the tested non-linear operators. Al-Regib and Ni in [35] used a non-linear energy operator for detecting the onset of chatter. Similarly, Caliskan et al.in [36] exploited a dimensionless chatter indicator based on a non-linear energy operator NEO. The chatter related contribution was filtered using the Kalman algorithm. The methodology is particularly suitable for complex cases characterized by multiple chatter frequencies, although some false alarms were observed when the tool is not engaged in the workpiece. Cao et al. in [37] developed a chatter detection system based on the self-organizing map SOM neural network. The methodology exploited, among several features extracted from the vibrational signals, three non-linear features. The conceived methodology seemed working although a critical learning phase was required.

Although some of the analyzed researches presented monitoring solutions that can be adapted to the on-line implementation, only few works really developed an integrated solution that efficiently detects and suppresses chatter vibrations. This is the case of Faassen in [38] and Dijk et al. [39] that used sophisticated monitoring techniques (i.e. $Box - Jenkins$) for real-time estimating the chatter frequency and consequently for defining the control action. This methodology, and similarly all the analyzed approaches, were conceived for applications in which the cutting speed is mainly kept constant during cutting. As a consequence, they would not be generally and profitably implemented in cutting vibration controllers that typically need to recursively change the spindle speed for finding stable cutting regions or even to implement the SSV chatter suppression technique.

Due to this literature lack, in this work a chatter detection algorithm, suitable for being used even under variable speed machining, was developed. For developing such a chatter detection methodology the cyclostationarity theory (Napolitano in [40] and in [41]) has been exploited. This methodology is particularly suitable for non stationary processes and it was successfully used is several fields, ranging from communications to mechanical applications, Antoni et al. in [42] and Raad et al. in [43]. Although this approach has been successfully used for fault detection in rotating machines, only two researches connected to chatter have been found, Lamraoui et al. in [44] and in [45]. More in details, in these works, the authors used an indicator based on *cyclostationary* for detecting chatter in milling but they limited its use to constant spindle speed CSM machining.

In the present paper, the methodology has been for the first time extended to variable speed regime and adapted to a real-time implementation. Procedures for automatically set the chatter threshold were also devised. The conceived chatter detection algorithm was tested with success in different conditions, including stable and unstable cutting, both at CSM and VSM.

The paper is structured as follows. In section 2, the main limitations of the existing approaches are illustrated exploiting cutting examples and the new algorithm development is explained. Section 3 describes the experimental set-up used for the final tests and the chatter detection performances are critically analyzed. In section 4, conclusions are outlined.

Nomenclature

α index of the set of periodic frequencies

$\boldsymbol{\nu}$ spindle speed fluctuation

$\boldsymbol{e}\left(\theta\left[n\right]\right)$ residuals from synchrnonous averaging process

$\boldsymbol{s}(\boldsymbol{t})$ generic signals associated to a stochastic process

$\boldsymbol{s}(\theta)$ vibrational signal in angular domain

$\boldsymbol{s}_b(\theta)$ contribution related to the noise in the angular domain

$\boldsymbol{s}_c(\theta)$ contribution related to chatter in the angular domain

$\boldsymbol{s}_p(\theta)$ contribution related to the milling periodicity in the angular domain

$\boldsymbol{s}_{air-cutting}(\theta)$ vibrational signal acquired during $air-cutting$ as function of the spindle angle θ

$\boldsymbol{t}$ used for defining a stochastic process

$\Delta\theta$ angular resolution

ΔT duration of time window used for the indicator $NICS2$ computation

Δt updating $NICS2$ period

$\hat{\boldsymbol{s}}_b(\theta)$ estimation of the contribution related to noise in the angular domain

$\hat{\boldsymbol{s}}_p(\theta)$ estimation of the contribution related to the milling periodicity in the angular domain

$\hat{\sigma}_{i_q}$ estimation of the standard deviation of $i_q(t)$

$\hat{\sigma}_{NICS2}$ estimation of the standard deviation of $NICS2$

$\hat{C}^{\alpha}_{1\boldsymbol{s}}$ estimator of the first order *cumulant*

$\hat{C}^{\alpha}_{2\boldsymbol{s}}(0)$ estimator of the second order *cumulant* at *lag* zero

$I\hat{C}S_{1\boldsymbol{s}}(t(j))$ first order estimator of *cyclostationarity*

$I\hat{C}S_{2\boldsymbol{s}}(t(j))$ second order estimator of *cyclostationarity*

Ω spindle speed

$\overline{\boldsymbol{s}(\theta(n))}$ average of the vibrational signal in the angular domain

$\overline{NICS2}$ average value of $NICS2$ calculated considering air-cutting

τ moving window delay

Θ tool revolution

θ spindle angle

$A3$ tabulated constant for the UCL calculation

a_e radial depth of cut

a_p axial depth of cut

$a_x(t)$, $a_y(t)$, $a_z(t)$ spindle acceleration along X, Y and Y directions

B_4 tabulated constant for the $UCL_{engagement}$ computation

$C_{1\boldsymbol{s}}(t)$ $first\ order\ cumulant$

$C_{2\boldsymbol{s}}(\boldsymbol{t})$ *second order cumulant*

$C_{h\boldsymbol{s}}(\boldsymbol{t})$ h^{th} $order\ cumulant\ function$

combined $NICS2$ combination of $NICS$ along X and Y direction

E *ensemble average*

f frequency

$f(n)$ instantaneous spindle speed frequency

f_s	sampling frequency
f_z	feed per tooth
f_{SSV}	frequency of the $SSSV$
g	number of samples of the moving window of ΔT
h	momentum order
$i_q(t)$	quadrature spindle motor current as a function of time
K	number of considered periods used in the *synchronous averaging* process
K_{ac}	axial shearing cutting coefficient
K_{ae}	axial edge cutting coefficient
K_{rc}	radial shearing cutting coefficient
K_{re}	radial edge cutting coefficient
K_{tc}	tangential shearing cutting coefficient
K_{te}	tangential edge cutting coefficient
l	number of considered samples for the $UCL_{engagement}$ computation
$m_{\boldsymbol{s}}$	$first - order\ momentum$
N	number of points per tool revolution used for the *order tracking*
n	n^{th} generic sample
$NICS2$	normalized chatter indicator
P	number of samples used for the indicators computation
$p_{\boldsymbol{s}}$	probability density function of the stochastic process $\boldsymbol{s}(t)$
q	number of samples used for the UCL computation
$r(t)$	windows that moves along the record trough the delay τ
$R_{2\boldsymbol{s}}(t_1, t_2)$	$second{-}order\ momentum$
RVA	dimensionless parameter for describing the amplitude of $SSSV$
$S(f,\tau)$	spectral components of s as a function of time t
$s(t)$	generic vibrational signal as a function of time t
$s_1, \ldots, s_n$	random variable of $\boldsymbol{s}(t)$
$S_b(f,\tau)$	spectral components of s related to noise as function of time t
$S_c(f,\tau)$	spectral components of s related to chatter a function of time t
$S_p(f,\tau)$	spectral components of s related to the periodicity of milling as a function of time t
$SS(t)$	spindle speed as a function of time t in revolution per minute rpm
SS_0	nominal spindle speed in revolution per minute rpm
SS_A	amplitude of the sine used in the $SSSV$ modulation in revolution per minute rpm
T	period of a cyclostationary process

t time

$t_1, \ldots, t_n$ realizations of $\boldsymbol{t}$

UCL upper confidence limit of the control chart, conceived for the chatter indicator

$UCL_{engagement}$ upper confidence limit for the control chart used for detection the tool-workpiece engagement

$Var\{\hat{C}^{\alpha}_{2\boldsymbol{s}}(0)\}$ variance of $\hat{C}^{\alpha}_{2\boldsymbol{s}}(0)$

2. Materials and Methods

2.1. Limitations of most of the literature approaches

Most of the analyzed chatter detection methodologies (i.e. the approaches based on the time-frequency analysis) fails into dealing with machining operations performed under variable spindle speed regime. This happens because they are based on the separation of the process-related frequencies (synchronous components linked to the spindle frequency and to the tooth passing frequencies S_p) from the chatter-related frequencies (typically called asynchronous components S_c) and the noise-related contribution S_b.

Since the spindle speed is varying, this separation can not be profitably performed. Moreover, the variation of the spindle speed typically involves complex modulation phenomena ([4]) that are difficultly investigated using classical techniques. This was demosntrated applying the $STFT$ (Equation 1, Randal [46]) to different cases:

- stable machining operation at constant speed machining CSM
- unstable milling operation carried out at constant speed machining CSM
- unstable milling operation with SSV.

$$S(f,\tau) = \int_{-\infty}^{\infty} s(t)r(t-\tau)e^{-j2\pi ft}dt = S_p(f,\tau) + S_c(f,\tau) + S_b(f,\tau) \qquad (1)$$

$s(t)$ is the time domain vibrational signal (i.e. spindle acceleration), $r(t)$ is a window that moves along the record through τ, f is the generic considered frequency and $S(f,\tau)$ is the result of the $STFT$ transform. As can be observed in Figure 1, for stable cutting at CSM, the tooth passing frequency TPF (61 Hz) and its higher order harmonics S_p can be clearly observed.

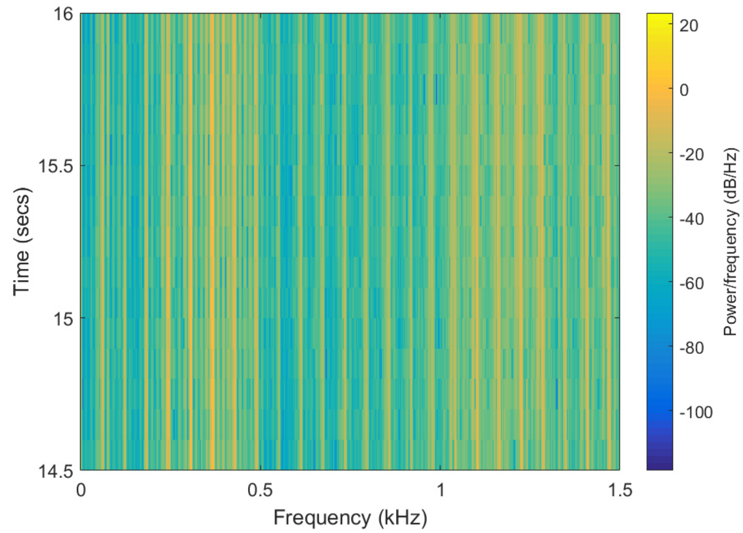

Figure 1: $STFT$, $S(f,\tau)$ of a stable machining at CSM

The time-frequency analysis can be used, with the limitations described the section 1, even for unstable cases at CSM. Indeed, in Figure 2 the chatter-related frequency S_c (400 Hz) is clearly visible.

This in not true in case of variable speed machining VSM. For instance, Figure 3 shows that an unstable SSV milling operation $S(f,\tau)$ has a more complex frequency structure and both the $S_p(f,\tau)$ and the $S_p(f,\tau)$ can not be easily appreciated. Moreover, if we focus on the frequency range close to 400 Hz, it seems that much more components are involved in the spectrogram making the stability assessment not feasible. This could be related to the already described modulation phenomena.

This example underlines the limitations of all the time-frequency approaches in the analysis of the complex phenomena involved when the the spindle speed is modulated or continuously changed.

In order to overcome these drawbacks, a chatter detection algorithm in the tool angular domain that exploits the cyclostationarity theory was developed. This theory is particularly suitable in presence of frequency modulations that typically affects the rotating machines.

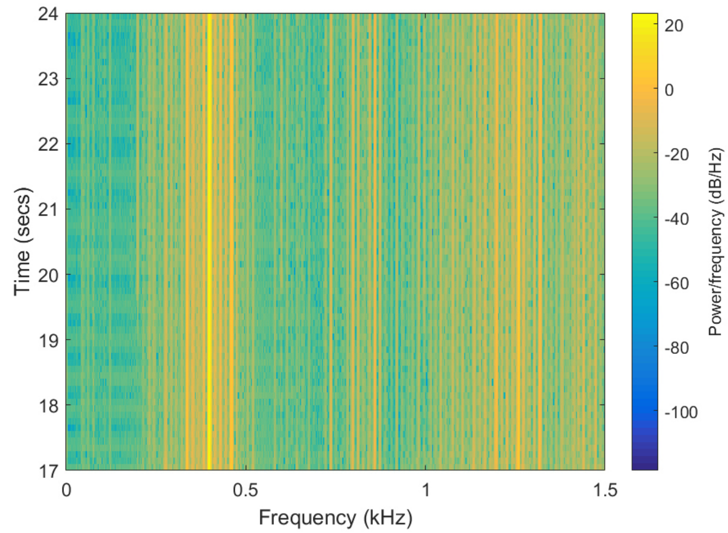

Figure 2: $STFT$, $S(f, \tau)$ of an unstable machining at CSM

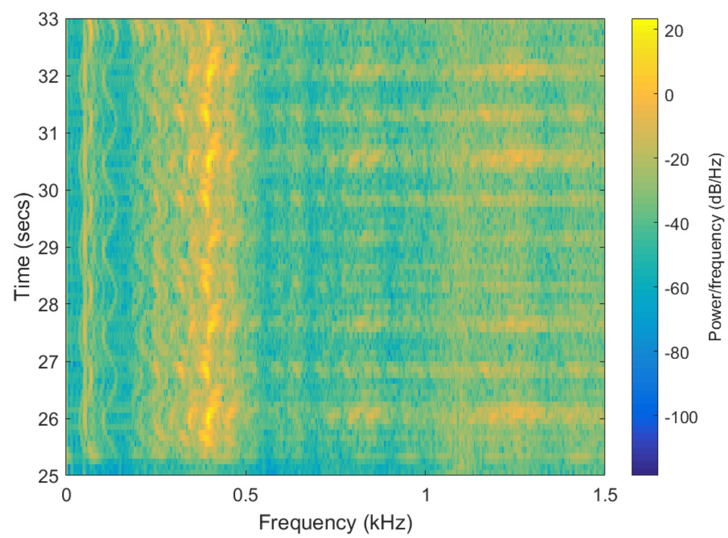

Figure 3: $STFT$, $S(f, \tau)$ of an unstable machining using SSV

2.2. Chatter detection algorithm development

As reported by Antoni et al. [42], cyclostationarity deals with stochastic processes $\{\boldsymbol{s}(\boldsymbol{t})\}_{\boldsymbol{t}\in\mathbb{R}}$ that show hidden periodicities. If the probability density function p of a stochastic process is periodic (Equation 2) in t with period T it can be defined $strict-sense\ cyclostationary$. It is worth of noting that $\boldsymbol{t}$ could stand for *time* or whatever generic variable, for instance the angle θ that can be used for describing the angular coordinate of rotating machines.

$$p_{\boldsymbol{s}}\left(s_1,\ldots,s_n;t_1,\ldots,t_n\right)=p_{\boldsymbol{s}}\left(s_1,\ldots,s_n;t_1+T,\ldots,t_n+T\right) \tag{2}$$

According with the application, the involved signals can show different kinds of cyclostationarity. For instance, if Equation 3 is satisfied, $\boldsymbol{s}$ is $first\ order\ cyclostationary\ (CS1)$.

$$m_{\boldsymbol{s}}\left(t\right)=E\{\boldsymbol{s}(t)\}=m_{\boldsymbol{s}}\left(t+T\right) \tag{3}$$

where E is the *ensemble average* and $m_{\boldsymbol{s}}$ the $first-order\ momentum$. If the second $second-order\ momentum$ (i.e. the $auto-correlation$ function $R_{2\boldsymbol{s}}\left(t_1,t_2\right)$) is periodic, $\boldsymbol{s}$ is $second\ order\ cyclostationary\ (CS2)$, Equation 4.

$$R_{2\boldsymbol{s}}\left(t_1,t_2\right)=E\{\boldsymbol{s}^*\left(t_1\right)\boldsymbol{s}\left(t_2\right)\}=R_{2\boldsymbol{s}}\left(t_1+T,t_2+T\right) \tag{4}$$

Signals with periodic amplitude or with frequency modulation fulfil the $CS2$ property. Signals that are both $CS1$ and $CS2$ are $wide-sense$ *cyclostationary*. The *cyclostationarity* property can be extended to the higher order momentum. In that case the general concept of h^{th} *order cyclostationary* (CSh) can be introduced.

In order to avoid that a generic signal is classified as (CSh) only because it inherited the property from the h^{th-1} *order* momentum (this is the typical case of periodic signals $\boldsymbol{s}(t)$) the h^{th} $order\ cumulant\ functions$ $C_{h\boldsymbol{s}}(\boldsymbol{t})$ can be introduced. For instance, the first and second order *cumulants* can be defined as follows, Equation 5 and Equation 6.

$$Cum\left[\boldsymbol{s}(t)\right]\triangleq C_{1\boldsymbol{s}}(t)\triangleq m_{\boldsymbol{s}}\left(t\right) \tag{5}$$

$$Cum\left[\boldsymbol{s}(t_1),\boldsymbol{s}(t_2)\right]\triangleq C_{2\boldsymbol{s}}(t_1,t_2)\triangleq R_{2\boldsymbol{s}}\left(t_1,t_2\right)-m_{\boldsymbol{s}}^*(t_1)m_{\boldsymbol{s}}(t_2) \tag{6}$$

The periodicity of the *cumulants* assures the property of *pure cyclostationary* of $\boldsymbol{s}$.

In spindle systems, as well as in the majority of the rotating machines, the signals are periodic with respect to the shaft rotation angle θ and, as a consequence, the signals are intrinsically $angle - cyclostationary$. It was demonstrated by Antoni et al. [42] that the $wide - sense\ cyclostationary$ of $\boldsymbol{s}$ is assured in both the angle θ and time t domains if and only if the speed fluctuation $\boldsymbol{\nu}(t)$ of the nominal spindle speed Ω (Equation 7) is itself $wide - sense\ cyclostationary$.

$$t \mapsto \theta(t) = \Omega \cdot t + \int_{-\infty}^{t} \boldsymbol{\nu}(u)\, du \tag{7}$$

For sake of generality, in order to assure the applicability of the *cyclostationarity*, it was decided to perform the vibrational analysis in the *angle* domain. In such a way, the methodology can be properly used even if the the spindle speed is changed without a specific periodic scheme (i.e. $SSSV$). This even allows preserving the periodicity of some process-related phenomena like the passing of the teeth.

In order to be able to carry out such analysis, it was performed a re-sample of the $\boldsymbol{s}(t)$ with respect to the spindle encoder signal $\theta(t)$ through the $cumputed\ order - tracking$, refer to Fyfe and Munck in [47] and Borghesani et al. [48].

For doing this, the tachometer reference signal is necessary. By subsequent interpolation steps, the tachometer signal (θ vector) was first reconstructed and successively interpolated considering $N = 1000$ equally-angularly spaced points ($\Theta = 2\pi = N \cdot \Delta\theta$) for each tool revolution. For each of this point, the corresponding data in time domain was founded and therefore the original signal (acceleration signals $\boldsymbol{s}(t)$) were represented in the *angle* domain $\boldsymbol{s}(\theta)$.

Once the order tracking is completed, the synchronous averaging operation (Equation 9) is performed in order to separate the periodic part $\boldsymbol{s}_p(\theta)$, the asynchronous part of the signal $\boldsymbol{s}_c(\theta)$ (typically related to chatter in unstable cutting conditions) and the noise-related contribution $\boldsymbol{s}_b(\theta)$ that generally affects the sensor acquisition, Equation 8. This is a preparatory operation that allows the further calculation of the chatter indicator that relies on the *cyclostationary* theory.

$$\boldsymbol{s}(\theta) = \boldsymbol{s}_p(\theta) + \boldsymbol{s}_c(\theta) + \boldsymbol{s}_b(\theta) \tag{8}$$

$$\hat{\boldsymbol{s}}_p\left(\theta\left[n\right]\right) = \frac{1}{K}\sum_{k=0}^{K-1}\boldsymbol{s}\left(\theta\left[m + k\cdot N\right]\right) \tag{9}$$

n is the number of the generic *sample* of $\boldsymbol{s}$, N is the number of considered *samples* for each period (*tool revolution* $\Theta = 2\pi = N \cdot \Delta\theta \rightarrow \Delta\theta = 2\pi/N$) and K the number of considered periods used for the averaging process. $m = n - \lfloor \frac{n}{N} \rfloor N$ and $\lfloor \frac{n}{N} \rfloor$ is the biggest whole number less or equal to the ratio n/N.

The contribution due to the noise $\hat{\boldsymbol{s}}_b(\theta)$ is estimated using the same averaging approach but considering a portion of the vibrational signals acquired during $air - cutting$ phase ($\boldsymbol{s}_{air-cutting}(\theta)$), that is before the tool engages the workpiece.

The tool-workpiece detection was accomplished using a control chart (Montomery [49]) on the variance of the *quadrature current* $i_q(t)$ absorbed by the spindle motor. For the considered spindle motor, the current $i_q(t)$ is proportional to the spindle *torque*. In particular, the upper confidence limit $UCL_{engagement}$ of the chart, used for detecting the tool engagement, was computed using Equation 10.

$$UCL_{engagement} = B_4(l) \cdot \hat{\sigma}_{i_q} \tag{10}$$

$\hat{\sigma}_{i_q}$ is the estimation of the *standard deviation* of the spindle current and B_4 is a tabulated value that depends on the number of samples l considered. In this case $l = 7$ samples were considered.

The estimation of the contribution due to chatter, that would be relevant for unstable cutting, can be performed computing the signal residuals $\boldsymbol{e}$, Equation 11.

$$\hat{\boldsymbol{s}}_c\left(\theta\left[n\right]\right) \simeq \boldsymbol{e}\left(\theta\left[n\right]\right) = \boldsymbol{s}\left(\theta\left[n\right]\right) - \hat{\boldsymbol{s}}_p\left(\theta\left[n\right]\right) - \hat{\boldsymbol{s}}_b\left(\theta\left[n\right]\right) \tag{11}$$

Considering the *cyclostationary* theory, a normalized chatter indicator ($NICS2$ in Equation 12) that compares, in the *angle* domain, the *cyclic power* related to the chatter contribution (estimated through the consistent estimator $I\hat{C}S_{2\boldsymbol{s}}$ reported at the numerator) and the one associated to the whole signal $\boldsymbol{s}$ (reported at the denominator), was computed. The indicator was derived from the research developed by Raad et al. in [43]. It was similarly used in Laraoui et al. [44] although, in that work, it was not tested in VSM and the indicator was not conceived for $real - time$ implementations.

In this research, the chatter detection indicator is updated every $t(j) - t(j-1) = \Delta t = 0.1\,\mathrm{s}$ and a moving window of $\Delta T = 0.3\,\mathrm{s}$ duration was considered for the $NICS2$ computation. Indeed, since the nature of chatter development in machining operations, an approach that considers a partially overlapped moving windows of $0,3\,\mathrm{s}$ was found a good compromise for its fast and robust detection.

$$NICS2\,(t(j)) = 100\frac{I\hat{C}S_{2\boldsymbol{s}}\,(t(j))}{\left(I\hat{C}S_{1\boldsymbol{s}}\,(t(j)) + I\hat{C}S_{2\boldsymbol{s}}((t(j))\right)} \tag{12}$$

According to Raad et al. [43], $I\hat{C}S_{1\boldsymbol{s}}$ and $I\hat{C}S_{2\boldsymbol{s}}$ are two consistent and normalized estimators conceived for measuring the "degree of cyclostationarity" of a stochastic process $\boldsymbol{s}$. In particular, $I\hat{C}S_{1\boldsymbol{s}}$ refers to $CS1$ and $I\hat{C}S_{2\boldsymbol{s}}$ to $CS2$ property of $\boldsymbol{s}$.

The $I\hat{C}S_{n\boldsymbol{s}}$ estimators are respectively defined in Equation 13 and Equation 14.

$$I\hat{C}S_{1\boldsymbol{s}}\,(t(j)) = \sum_{\alpha\in f,\alpha\neq 0} \frac{\left|\hat{C}^{\alpha}_{1\boldsymbol{s}}\,(t(j))\right|^2}{\left(Var\{\hat{C}^{\alpha}_{2\boldsymbol{s}}(0)\}\,(t(j))\right)} \tag{13}$$

$$I\hat{C}S_{2\boldsymbol{s}}\,(t(j)) = \sum_{\alpha\in 2\pi f,\alpha\neq 0} \frac{\left|\hat{C}^{\alpha}_{2\boldsymbol{s}}(0)\,(t(j))\right|^2}{\left(Var\{\hat{C}^{\alpha}_{2\boldsymbol{s}}(0)\}\,(t(j))\right)^2} \tag{14}$$

$\hat{C}^{\alpha}_{1\boldsymbol{s}}$ and $\hat{C}^{\alpha}_{2\boldsymbol{s}}(0)$ are the consistent estimators of the first and second order *cumulants* at *lag* zero. In such a way, they allows considering all the spectral information of a *cyclostationary* signal, Raad et al. [43]. α is the index of the periodic frequencies.

Considering the conceived chatter indicator $NICS2$, $\hat{C}^{\alpha}_{1\boldsymbol{s}}$ and $\hat{C}^{\alpha}_{2\boldsymbol{s}}(0)$ can be respectively computed through Equation 15 and Equation 16.

$$\hat{C}^{\alpha}_{1\boldsymbol{s}}\,(t(j)) = P^{-1}\sum_{n=0}^{P-1} \hat{\boldsymbol{s}}_p\,(\theta\,[n])\,e^{-j2\pi n f(n)\Delta\theta} \tag{15}$$

$$\hat{C}^{\alpha}_{2\boldsymbol{s}}(0)\,(t(j)) = P^{-1}\sum_{n=0}^{P-1}\hat{\boldsymbol{s}}_c\,(\theta\,[n])\,e^{-j2\pi nf(n)\Delta\theta} = P^{-1}\sum_{n=0}^{P-1}\boldsymbol{e}\,(\theta\,[n])\,e^{-j2\pi nf(n)\Delta\theta} \tag{16}$$

$$Var\{\hat{C}^{\alpha}_{2\boldsymbol{s}}(0)\}\,(t(j)) = P^{-1}\sum_{n=0}^{P-1}\Big(\boldsymbol{s}\,(\theta(n)) - \overline{\boldsymbol{s}\,(\theta(n))}\Big) \tag{17}$$

It is worth of noting that the process-related part $\hat{\boldsymbol{s}}_p$ was used for computing $\hat{C}^{\alpha}_{1\boldsymbol{s}}$ and the residual part connected to chatter $\hat{\boldsymbol{s}}_c$ for the $\hat{C}^{\alpha}_{2\boldsymbol{s}}$ calculation. Moreover, according to Equation 12, the normalized $NICS2$ indicator ranges from 0 to 100.

The *variance* $Var\{\hat{C}^{\alpha}_{2\boldsymbol{s}}(0)\}$ is used for normalizing the indicator $I\hat{C}S_{n\boldsymbol{s}}$, Equation 17. $\overline{\boldsymbol{s}\,(\theta(n))}$ is the average of P samples of the considered signals $\boldsymbol{s}$. $f(n)$ is the instantaneous spindle speed frequency.

All the terms used for estimating the chatter indicator $NICS2$ (Equation 15, Equation 16 and Equation 17) are updated every Δt. These terms are computed in the *angle* domain, just after the implementation of the *order tracking* and the *synchronous averaging*, considering a moving windows $\Delta T = t(j+g) - t(j) = 0.3\,\mathrm{s}$. As already mentioned, the order tracking is based on the signal angular re-sample with an equally spaced angular vector ($\Delta\theta = 2\pi/1000$) that makes the algorithm processing P elements in the considered window ΔT, Equation 18. For what concerns the *synchronous averaging*, $K = P/N$ is the number of tool revolutions used for filtering the process-related components. For the analyzed cases (reported in Section 3.1), $K = 4$.

$$P = \lfloor\frac{\theta\,(t(j+g)) - \theta\,(t(j))}{2\pi}\rfloor \cdot N \tag{18}$$

The adopted settings (ΔT, Δt, N and consequently P and K) assured a good compromise between the averaging process, the capability of detecting fast changes in the cutting conditions and the computational effort.

The explained chatter detection algorithm can be resumed in Figure 4. The algorithm processes the spindle encoder (tachometer), the vibrational signals (in this case the spindle nose acceleration) and the spindle current i_q, both acquired at the sampling frequency $f_s = 10k\,\mathrm{Hz}$, and provides and indication of chatter through the $NICS2$ estimation. The blocks that implement the signals processing, the order tracking and the *synchronous averaging*, are clearly visible on the left side of the picture. They adopt Equations 8, 9 and 11. The chatter indicator computation is performed by the three blocks reported at the centre of the picture. The tool-workpiece detection is provided by the block (Equation 10) reported at the top of the scheme. In order to perform a chatter assessment, the $NICS2\left((j)\right)$ indicator is compared with a threshold UCL that is computed exploiting the theory of control charts (Montomery [49]) for the mean of $\overline{NICS2}$, Equation 19.

$$UCL = \overline{NICS2} + A3(q) \cdot \hat{\sigma}_{NICS2} \tag{19}$$

$A3(q)$ is a tabulated value that depends on the number of considered samples q (in this case $q = 6$). The threshold is computed considering the $NICS2$ values calculated during air-cutting that is with the spindle put into rotation but before entering in the workpiece. It was decided to adopt this approach because it is quite simple and fast to calculate the corresponding threshold in combination with the already described tool-workpiece detection module. Indeed, this approach is particularly suitable when the threshold value needs to be frequently updated since the tool and the cutting set-up is changed during the production of complex workpieces.

3. Results and Discussion

3.1. Experimental set-up and validation tests definition

In order to test the capability of the developed indicator into detecting chatter vibration, several milling tests involving non-constant speed cutting were performed. The tests were carried out on a 4 axis *Mandelli M5* machine, equipped with a *Capellini* hydrostatic electro-spindle (160 Nm, 7000 rpm). The spindle is fully sensorized for measuring process-related vibrations. More specifically, an inner tri-axial accelerometer (100 mV/g) is located in the spindle housing, close to the front bearings (spindle nose). Moreover, two eddy current displacement sensors measure the relative displacement between the spindle housing and the rotating shaft. A monitor system based on *National Instruments* real time platform *PXI* was used to acquire sensors data (with a sampling frequency of $f_s = 10k$ Hz) and to compute the developed chatter indicator. Moreover, the monitoring system processes the signal coming from the angular encoder installed on the spindle. The *PXI* platform was also used to set the cutting parameters (mainly the

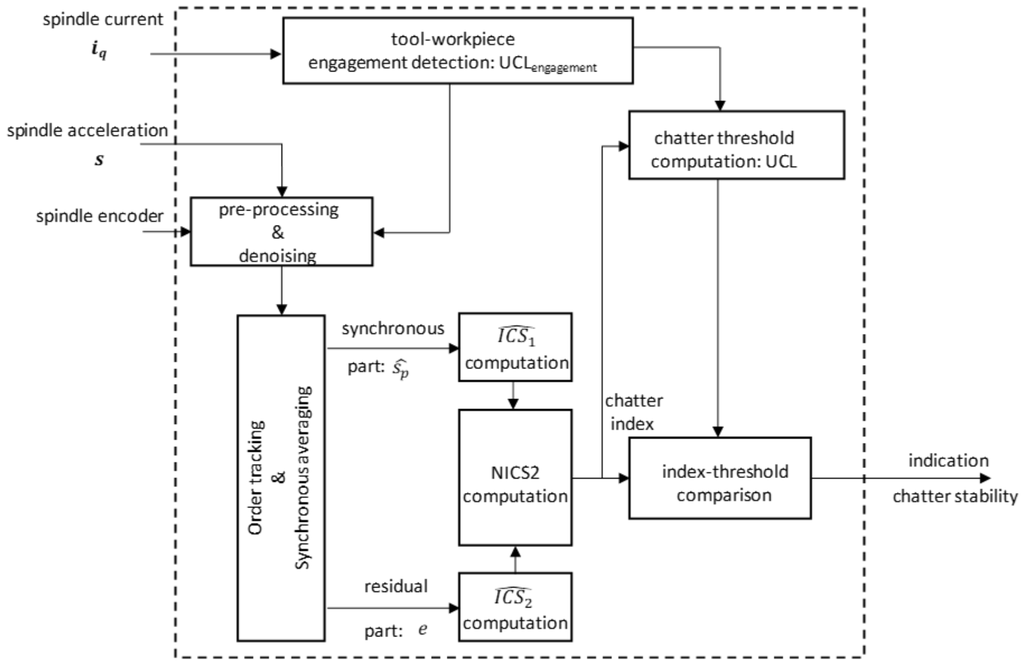

Figure 4: Developed chatter detection methodology description

spindle speed) during the tests. A scheme of the adopted set-up is reported in Figure 5.

More in detailed, in this research, the control unit was used for setting the desired spindle speed or for continuously modulating it. It is worth of noting that, in this research, the real-time platform was not used for closing the loop control but just for setting the desired spindle working speed. In this research the closed loop performances in terms of chatter suppression have not been investigated. The focus is on the capabilities of the developed chatter monitoring algorithm.

The cutting tests were carried out using an 80 mm tool with four equally-spaced inserts ($Sandvik - Coromant$ $R390 - 17$ 04 $08E - NH13A$). $C45$ was the material processed during the milling tests.

Since it was necessary to test the chatter monitoring algorithm in different conditions (stable cutting, unstable cutting, CSM and variable spindle speed machining VSM (i.e. SSV)) for inferring about its robustness, a chatter stability analysis was performed for planning the tests.

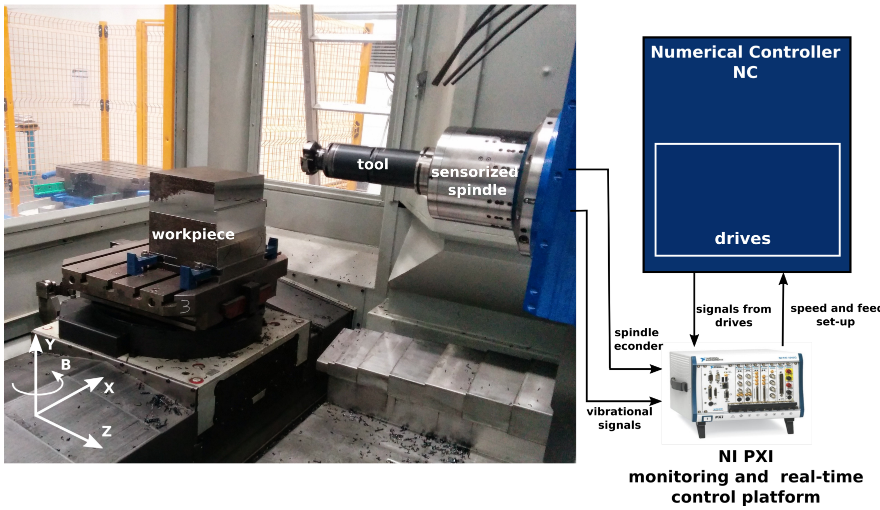

Figure 5: Experimental set-up: monitoring system

A tap test was carried out first. The experimentally measured tool tip dynamic compliance is reported in Figure 6.

Some cutting tests were performed in order to identify the cutting coefficients, Altintas in [50]. During the cutting tests the average cutting forces were measured through a $Kistler$ dynamometer ($9255B$) and the corresponding amplifier ($Kislter$ $5070A$). Several cutting conditions changing the feed per tooth f_z , the axial depth of cut a_p and spindle speed velocity were tested. The cutting coefficients (K_{tc}, K_{rc} and K_{ac} are respectively the tangential, the radial and the axial coefficients due to the shear, while K_{ec}, K_{ec} and K_{ec} are the edge contributions along the same directions). The identified cutting coefficients were summarized in Table 1.

Cutting coefficient	$K_{tc}\,[N/mm^2]$	$K_{rc}\,[N/mm^2]$	$K_{ac}\,[N/mm^2]$	$K_{te}\,[N/mm]$	$K_{re}\,[N/mm]$	$K_{re}\,[N/mm]$
Identified Value	1632.2	416.5	136.8	105.1	137.4	30.1

Table 1: Experimental cutting coefficients identification

The stability lobe diagram (Figure 7) was thus computed exploiting the $0-order$ approach (Altintas and Budak in [51]) and setting the radial depth of cut $a_e = 80\,\mathrm{mm}$ and the feed $fz = 0.15\,\mathrm{mm/tooth}$.

According to the insert feasible cutting speeds and the processed material, it was decided to perform the cutting tests in two regions of the stability

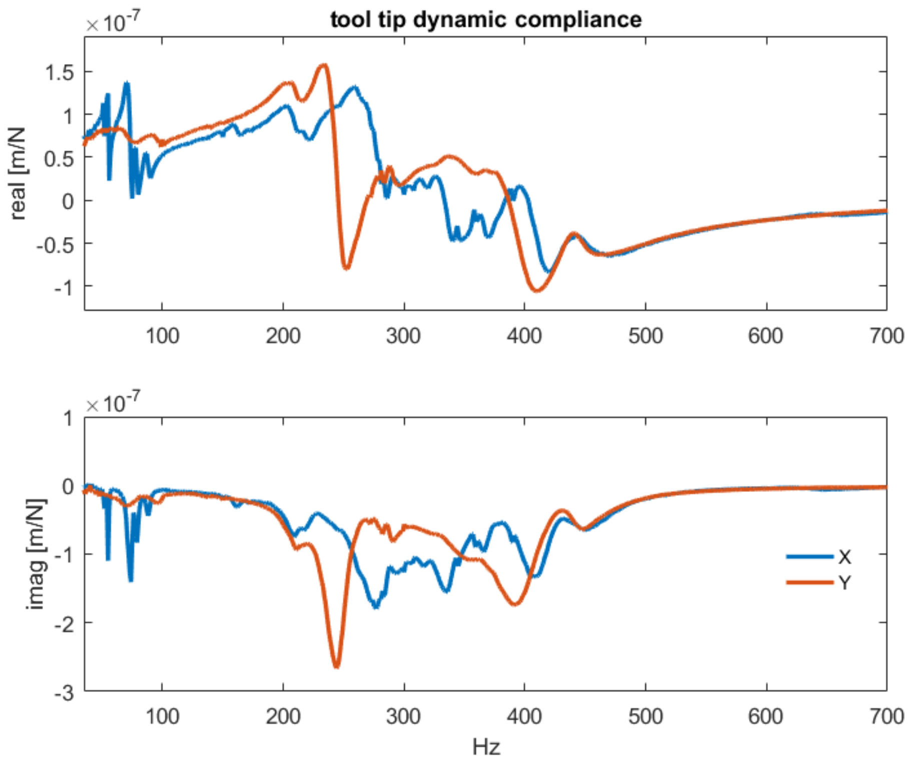

Figure 6: Measured tool tip dynamic compliance, X and Y direction

diagram, see the points reported Figure 7. Basically, all the cutting tests were performed with the axial depth of cut $a_p = 2.5\,\mathrm{mm}$ but using different average spindle speeds, that is $SS_0 = 876\,\mathrm{rpm}$ (used in $test-case$ 3) and $SS_0 = 914\,\mathrm{rpm}$ (used in $test-case$ 1 and $test-case$ 2). The selected milling conditions, if performed at CSM, are respectively characterized by a stable and an unstable cutting. In order to properly test the algorithm, in each $test-case$, the cutting speed SS was not kept constant to its nominal value SS_0 for the whole cut but, in the second part of the pass, it was modulated using the the $SSSV$. According to Equation 21 and Equation 20, the velocity was modulated using a *sine* of amplitude SS_A and frequency f_{SSSV}. RVA is the dimensionless parameter used for describing the speed modulation amplitude. More in details, for each $test-case$, the first part of the milling pass was executed at CSM up to a certain time, later on, the cutting were

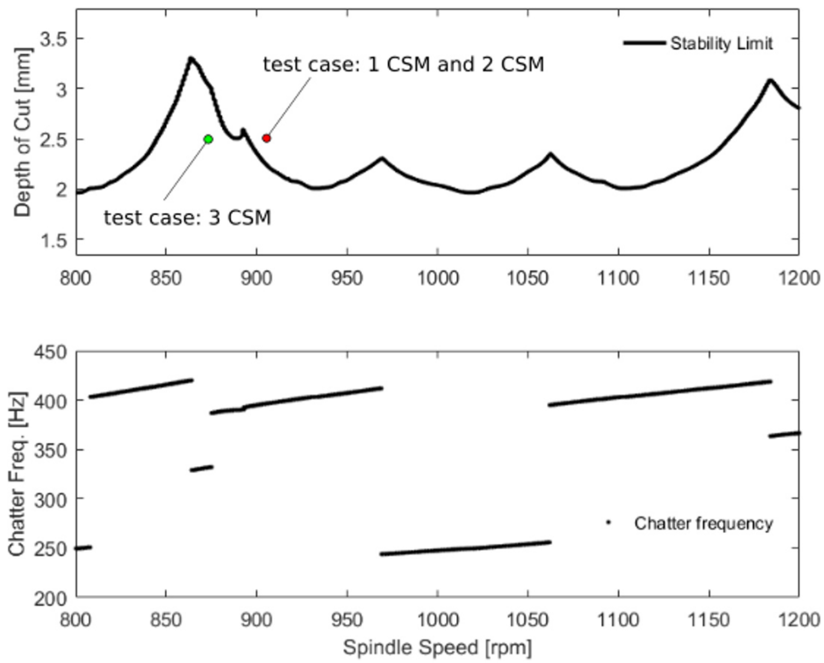

Figure 7: Stability Lobes Diagram and chatter frequencies

commutated to the $SSSV$ through the external controller that properly set the spindle speed SS reference to the machine drives, Figure 5.

$$RVA = SS_A/SS_0 \tag{20}$$

$$SS(t) = SS_0 \cdot (1 + RVA) \cdot sin(2 \cdot \pi \cdot f_{SSSV} \cdot t) \tag{21}$$

The cutting conditions used for the validation of the chatter monitoring algorithm are summarized in Table 2. The selection of the parameters of the SSSV was done referring both to the scientific literature (Zatarin et al. [52]) and to the results of preliminary cutting tests. During these preliminary tests, the capability of the SSSV of stabilizing an unstable cut or even the capability of destabilizing a stable cut were experimented.

The preliminary tests were used also for analyzing the capability of the spindle system of tracking the set speed reference.

test	first cut portion	last cut portion
$test-case$ 1	CSM (SS_0=914 rpm)	SSV (SS_0=914 rpm, RVA=0.1, f_{SSSV}=1.33 Hz)
cutting condition	unstable	stabilized by the SSSV
$test-case$ 2	CSM (SS_0=914 rpm)	SSV (SS_0=914 rpm, RVA=0.15, f_{SSSV}=0.67 Hz)
cutting condition	unstable	not stabilized by the SSSV
$test-case$ 3	CSM (SS_0=876 rpm)	SSV (SS_0=876 rpm, RVA=0.2, f_{SSSV}=0.67 Hz)
cutting condition	stable	destabilized by the SSSV

Table 2: Cutting tests used for the chatter monitoring algorithm validation

3.2. Chatter detection results

The developed chatter indicator was tested analyzing data coming from real milling tests. In particular, it was decided to compute the chatter indicator using the accelerations, both along X and Y directions $\boldsymbol{s}(t) = \{a_x(t), a_y(t)\}$, measured at the spindle house and sampled at $f_s = 10k$ Hz. For all the analyzed test cases, the conceived chatter indicator was computed and updated every $\Delta t = 0.1$ s. More specifically, an indicator (combined $NICS2$) is computed considering the average of the $NICS2$ values calculated both for a_x and a_y. For sake of generality, the $NICS2$ computation could be carried out considering even the contribution of the acceleration along the Z direction. Since the experimentation was performed executing face milling operations in the X-Y plane, in which, for the considered tool, the a_z acceleration is much lower than the contributions along the other directions, the indicator was calculated using Equation 22.

$$combined\ NICS2\,(t(j)) = \frac{NICS2_x\,(t(j)) + NICS2_y\,(t(j))}{2} \tag{22}$$

The chatter detection validation was performed comparing the combined $NICS2\,(t(j))$ indicator and the corresponding threshold UCL to the acceleration signal. Moreover, the $STFT$ of the acceleration and the machined surfaces were also used for assessing the cutting stability.

In $test-case$ 1, as reported in Table2, the first part of the pass (A and B) was carried out at CSM. Portion A refers to the tool-workpiece engagement where the radial immersion progressively increased causing the occurrence of chatter (portion B). The vibration growth can be observed in the acceleration a_x signal, upper picture of Figure 8 and in Figure 10 where the $STFT$ of whole $test-case$ 1 is reported. The $STFT$ of the unstable portion (B) was also reported in Figure 2. The main chatter frequency (400 Hz) that was properly predicted by the SLD theory (Figure 7) was clearly visible. In the third cutting portion (C), the adoption of $SSSV$ reduced significantly the vibrations. The forth portion (D) of the signal refers to the tool-workpiece disengagement in which the radial immersion varied during cutting.

The *combined* $NICS2$ chatter indicator is reported on the bottom picture of Figure 8.

As can be noted, the developed chatter monitoring methodology is able to detect both the presence of chatter (while CSM) and its suppression due to the introduction of the $SSSV$. It was demonstrated that the conceived indicator provided the right stability indication even when the cutting was non-stationary (i.e. portion D). Indeed, in such case both the radial depth of cut and the spindle speed were varying. The four cutting conditions can be clearly be appreciated in the $STFT$: workpiece engagement where progressively the cutting became unstable (A), the unstable cut (B), the transition from unstable to stable cutting due to the SSV implementation (C) and the disengagement phase (D). The *combined* $NICS2$ is also able to appreciate small fluctuations of the spindle acceleration caused (part C) by the introduced chatter suppression methodology. According to the pre-calculated threshold ($UCL = 57.2$), the process can be considered stable. As anticipated, the stability assessment was done analyzing the surface quality as well. For what concerns the stabilized cutting, the quality of the resulting surface can be appreciated at the centre of Figure 10. It can be noted that the surface quality is not so different from a stable operation performed at CSM (left side of Figure 10) and no chatter marks are visible on the workpiece although, some frequency components are still appreciable in a range centred on the chatter frequency. The observed spectral behaviour was even theoretically proven, Totis et al. [4].

The indicator exhibited a good performance even during the engagement/disengagement of the tool in the workpiece. It showed some issues only during the abrupt transition between the CSM and VSM cutting where a false chatter indication is provided but just for few samples. This is caused by a not optimized transition between CSM and the VSM regime. Indeed, a smoothing function for the spindle speed reference would be necessary to reduce this drawback but it was out the scope for this research.

In $test - case$ 2, the first portion (A and B) of the milling operation was executed in the same conditions as the previous case. Different $SSSV$ parameters were used for the last portion of the cut (C and D), Table 2. Indeed, the RVA was set to 0.15 and the f_{SSV} was reduced to 0.67 Hz. As can be observed in Figure 11, the $SSSV$ seems not definitely capable of

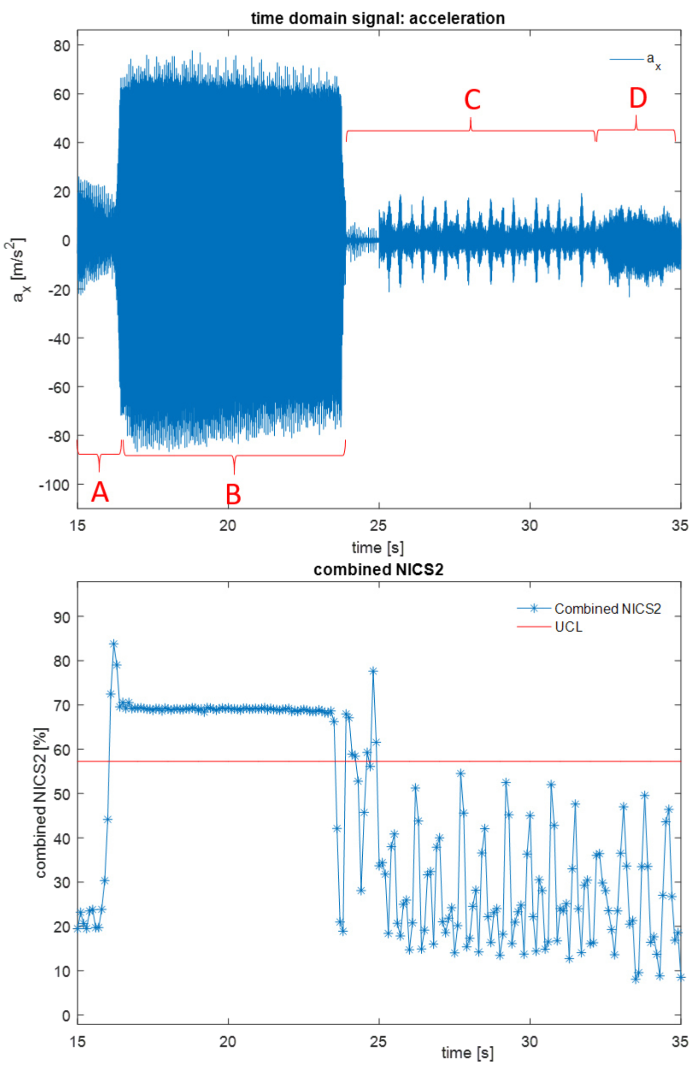

Figure 8: spindle house acceleration X direction (upper picture) and chatter indicator (bottom picture), $test - case$ 1

suppressing regenerative chatter. Indeed, some relevant vibration "blazes" can be clearly noted. The unacceptable chatter marks originated from the described "blazes" can be appreciated in Figure 10 (right side). At the same

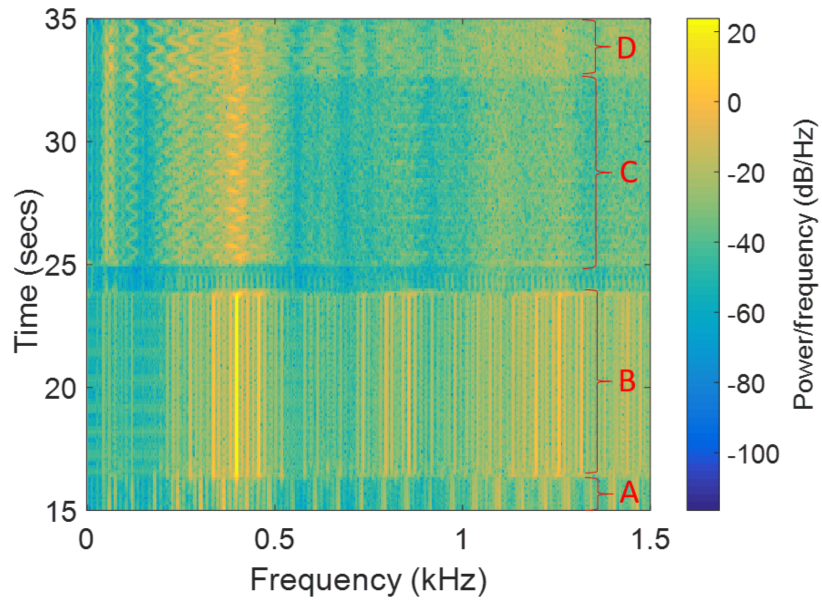

Figure 9: $STFT$, $S(f,\tau)$ of acceleration in $test - case$ 1

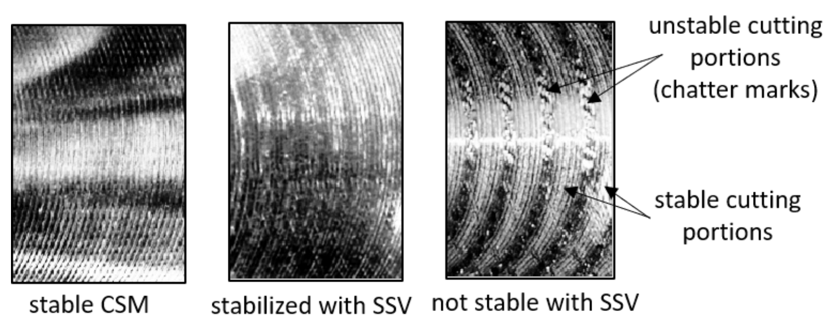

Figure 10: Surface quality in different cutting conditions (stable (left), stabilized with SSV (central) and unstable with SSV (right)

time, some portions of the cut seem stable. This phenomenon typically happens when the $SSSV$ strategy is not appropriate. The associated $STFT$ can be observed in Figure 12, portion C. It can be compared to the corresponding stabilized cutting studied in $test - case$ 1. In such case the involved frequen-

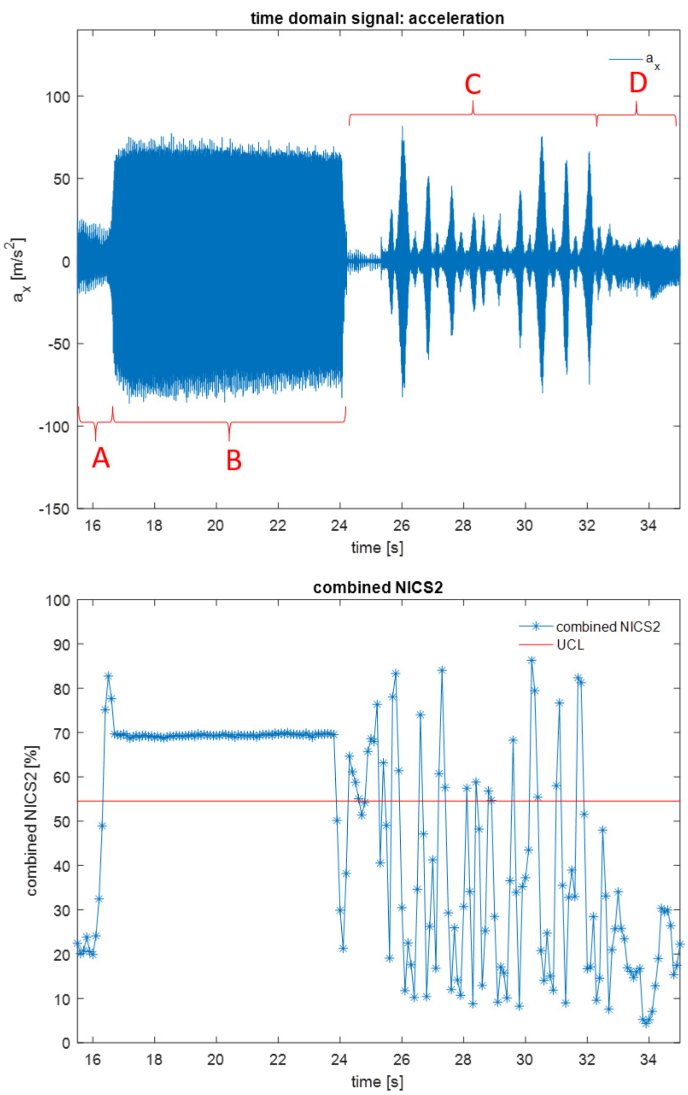

Figure 11: spindle house acceleration X direction (upper picture) and chatter indicator (bottom picture), $test - case$ 2

cies showed much lower amplitudes. Even in $test - case$ 2, the the conceived chatter indicator provided the right indication. Moreover, the capability of detecting such situations can be very useful especially if an adaptive implementation of the $SSSV$ is foreseen in a chatter control system. The $STFT$ of the acceleration reported in Figure 12 confirms the chatter detection performances of the conceived methodology. This is demonstrated even in the portions A and D. More specifically, when the tool was leaving the workpiece (D), the progressive reduction of the radial engagement made the cut stable and this behaviour was properly captured by the *combined* $NICS2$. In such condition the cut can be considered non-stationary since the radial engagement of the tool was decreasing while the spindle speed was varying according to the implemented SSV.

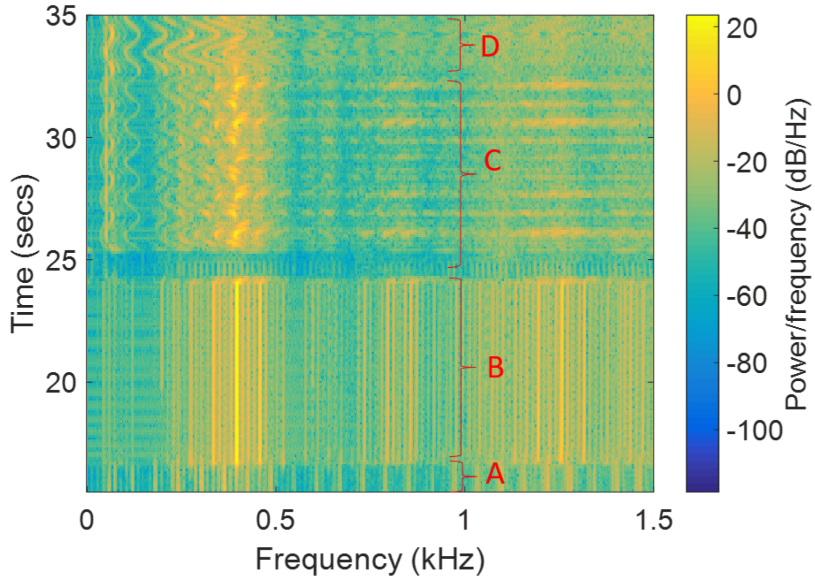

Figure 12: $STFT$, $S(f,\tau)$ of acceleration in $test-case$ 2

The vibration "blazes", upper side of Figure 11, shows that the conceived chatter indicator the *combined* $NICS2$ owns this specific skill although the "blazes" appear like a sequence of narrow pulses (Figure 11) that averagely last $0.15 - 0.30\,\text{s}$. In $test-case$ 2, the block that computes the chatter threshold exploiting the acceleration data referred to air cutting set it to $UCL = 54.5$ value.

In $test-case$ 3, a completely different scenario was considered. Indeed, the first portion of the cut was executed with parameters (Table 2) that assured stable cutting conditions, upper picture of Figure 13. It can be observed that the initial portion of the cut (A, B and C) was characterize by low vibrations. This was due to the fact that the selected nominal spindle speed matched one of the stability pockets of the stability chart, Figure 7. The surface quality associated to stable cutting at CSM is reported in Figure 10 (left side). In the last part of the cut the $SSSV$ was introduced. As a consequence, since a stable cutting condition was perturbed with the modulation of the spindle speed, chatter vibration occurred. Even in this case, the vibration blazes connected to unstable cutting were perfectly detected by the developed methodology. Indeed, the chatter indicator $NICS2$ fluctuations across the threshold UCL perfectly reproduce the fast alternation of stable and unstable conditions that characterizes some unstable milling operations performed with the SSV. The resulting machined surface was similar to the one reported in Figure 10 (right side). The effectiveness of the developed chatter detection methodology can be more clearly appreciated if the results achieved in $test - case$ 3 (second cut portion) are compared to the one reported in Figure 3 where, for the same data, the $STFT$ was applied without the possibility to easily assess the cutting stability, especially if real-time implementation is sought.

4. Conclusions

The development of a generalized chatter methodology for non-stationary milling operations was carried out in this research. The algorithm is suitable for an implementation as a real-time chatter detection in industrial conditions or even as a module of a chatter control system. The chatter indicator rely on the theory of the cyclostationarity and it was calculated in the spindle angle domain. The indicator was successfully tested in different machining conditions (stable, unstable, stabilized and un-stabilized cutting) and considering both constant or variable speed machining. For all the analyzed cases, the methodology showed good performance in terms of reliability and the capability of dealing with cutting conditions that fast evolve.

Acknowledgement

The present research was developed in the framework of a project ("CLUSTER: High Performance Manufacturing" - $CTN0100163216758$) founded by $MIUR$ (The Italian Ministry of Education and Research). Moreover, the

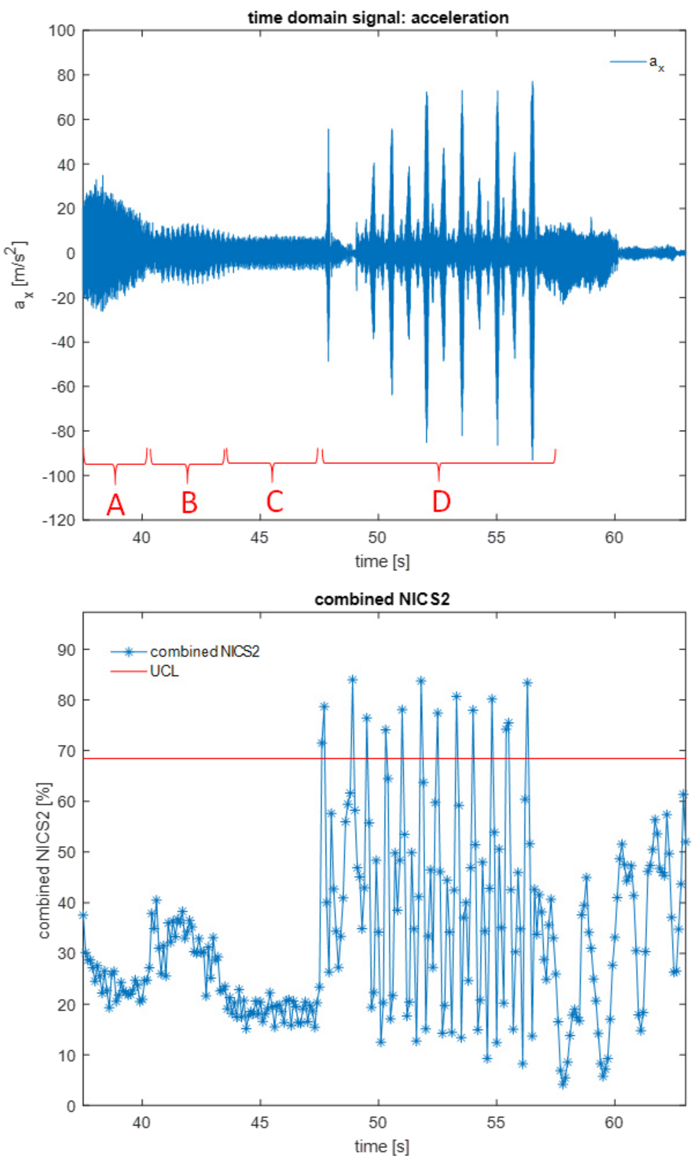

Figure 13: spindle house acceleration X direction (upper picture) and chatter indicator (bottom picture), $test - case$ 3

authors would thank the machine tool manufactured *Mandelli Sistemi* for the support.

References

[1] G. Quintana, J. Ciurana, Chatter in machining processes: A review, International Journal of Machine Tools and Manufacture 51 (2011) 363 – 376.

[2] J. Munoa, X. Beudaert, Z. Dombovari, Y. Altintas, E. Budak, C. Brecher, G. Stepan, Chatter suppression techniques in metal cutting, CIRP Annals 65 (2016) 785 – 808.

[3] Y. Altintas, M. Weck, Chatter Stability of Metal Cutting and Grinding, CIRP Annals - Manufacturing Technology 53 (2004) 619–642.

[4] G. Totis, P. Albertelli, M. Sortino, M. Monno, Efficient evaluation of process stability in milling with spindle speed variation by using the chebyshev collocation method, Journal of Sound and Vibration 333 (2014) 646 – 668.

[5] Y. Altintas, P. K. Chan, In-process detection and suppression of chatter in milling, International Journal of Machine Tools and Manufacture 32 (1992) 329 – 347.

[6] E. Soliman, F. Ismail, Chatter suppression by adaptive speed modulation, International Journal of Machine Tools and Manufacture 37 (1997) 355–369.

[7] F. Ismail, E. G. Kubica, Active suppression of chatter in peripheral milling part 1. a statistical indicator to evaluate the spindle speed modulation method, The International Journal of Advanced Manufacturing Technology 10 (1995) 299–310.

[8] H. Cao, X. Zhang, X. Chen, The concept and progress of intelligent spindles: A review, International Journal of Machine Tools and Manufacture 112 (2017) 21 – 52.

[9] T. L. S. M. Engineer, K. M. M. Engineer, B. D. I. Maker, Exploring once-per-revolution audio signal variance as a chatter indicator, Machining Science and Technology 6 (2002) 215–233.

[10] T. L. Schmitz, Chatter recognition by a statistical evaluation of the synchronously sampled audio signal, Journal of Sound and Vibration 262 (2003) 721–730.

[11] N.-C. Tsai, D.-C. Chen, R.-M. Lee, Chatter prevention for milling process by acoustic signal feedback, The International Journal of Advanced Manufacturing Technology 47 (2010) 1013–1021.

[12] G. Quintana, J. Ciurana, I. Ferrer, C. A. Rodríguez, Sound mapping for identification of stability lobe diagrams in milling processes, International Journal of Machine Tools and Manufacture 49 (2009) 203 – 211.

[13] D. Aslan, Y. Altintas, On-line chatter detection in milling using drive motor current commands extracted from {CNC}, International Journal of Machine Tools and Manufacture 132 (2018) 64 – 80.

[14] E. Kuljanic, M. Sortino, G. Totis, Multisensor approaches for chatter detection in milling, Journal of Sound and Vibration 312 (2008) 672 – 693.

[15] T. Insperger, G. Stépán, P. Bayly, B. Mann, Multiple chatter frequencies in milling processes, Journal of Sound and Vibration 262 (2003) 333 – 345.

[16] I. N. Tansel, M. Li, M. Demetgul, K. Bickraj, B. Kaya, B. Ozcelik, Detecting chatter and estimating wear from the torque of end milling signals by using index based reasoner (ibr), The International Journal of Advanced Manufacturing Technology 58 (2012) 109–118.

[17] R. Koike, Y. Kakinuma, T. Aoyama, K. Ohnishi, Evaluation of sensorless identification method for stable spindle rotation against chatter with milling simulation analysis, Procedia CIRP 46 (2016) 169 – 172. 7th HPC 2016–CIRP Conference on High Performance Cutting.

[18] H. Cao, Y. Yue, X. Chen, X. Zhang, Chatter detection based on synchrosqueezing transform and statistical indicators in milling process, The International Journal of Advanced Manufacturing Technology 95 (2018) 961–972.

[19] H. Cao, Y. Yue, X. Chen, X. Zhang, Chatter detection in milling process based on synchrosqueezing transform of sound signals, The International Journal of Advanced Manufacturing Technology 89 (2017) 2747–2755.

[20] Y. Wu, R. Du, Feature extraction and assessment using wavelet packets for monitoring of machining processes, Mechanical Systems and Signal Processing 10 (1996) 29 – 53.

[21] L. Wang, M. Liang, Chatter detection based on probability distribution of wavelet modulus maxima, Robotics and Computer-Integrated Manufacturing 25 (2009) 989 – 998. 18th International Conference on Flexible Automation and Intelligent Manufacturing.

[22] M. C. Yoon, D. H. Chin, Cutting force monitoring in the endmilling operation for chatter detection, Proceedings of the Institution of Mechanical Engineers, Part B: Journal of Engineering Manufacture 219 (2005) 455–465.

[23] T. Choi, Y. C. Shin, On-line chatter detection using wavelet-based parameter estimation., Transactions of the ASME, Journal of Manufacturing Science and Engineering 125 (2003) 21–28.

[24] Z. Zhang, H. Li, G. Meng, X. Tu, C. Cheng, Chatter detection in milling process based on the energy entropy of vmd and wpd, International Journal of Machine Tools and Manufacture 108 (2016) 106 – 112.

[25] N. E. Huang, Z. Shen, S. R. Long, M. C. Wu, H. H. Shih, Q. Zheng, N.-C. Yen, C. C. Tung, H. H. Liu, The empirical mode decomposition and the Hilbert spectrum for nonlinear and non-stationary time series analysis, Proceedings of the Royal Society of London A: Mathematical, Physical and Engineering Sciences 454 (1998) 903–995.

[26] Y. Fu, Y. Zhang, H. Zhou, D. Li, H. Liu, H. Qiao, X. Wang, Timely online chatter detection in end milling process, Mechanical Systems and Signal Processing 75 (2016) 668 – 688.

[27] Y. Ji, X. Wang, Z. Liu, Z. Yan, L. Jiao, D. Wang, J. Wang, Eemd-based online milling chatter detection by fractal dimension and power spectral entropy, The International Journal of Advanced Manufacturing Technology 92 (2017) 1185–1200.

[28] H. Cao, Y. Lei, Z. He, Chatter identification in end milling process using wavelet packets and hilbert–huang transform, International Journal of Machine Tools and Manufacture 69 (2013) 11 – 19.

[29] H. Cao, K. Zhou, X. Chen, Chatter identification in end milling process based on eemd and nonlinear dimensionless indicators, International Journal of Machine Tools and Manufacture 92 (2015) 52 – 59.

[30] S. Wan, X. Li, W. Chen, J. Hong, Investigation on milling chatter identification at early stage with variance ratio and hilbert–huang transform, The International Journal of Advanced Manufacturing Technology (2017).

[31] R. Rafal, L. Pawel, K. Krzysztof, K. Bogdan, W. Jerzy, Chatter identification methods on the basis of time series measured during titanium superalloy milling, International Journal of Mechanical Sciences 99 (2015) 196 – 207.

[32] D. Pérez-Canales, L. Vela-Martínez, J. C. Jáuregui-Correa, J. Alvarez-Ramirez, Analysis of the entropy randomness index for machining chatter detection, International Journal of Machine Tools and Manufacture 62 (2012) 39 – 45.

[33] L. Vela-Martínez, J. C. Jáuregui-Correa, J. Álvarez Ramírez, Characterization of machining chattering dynamics: An r/s scaling analysis approach, International Journal of Machine Tools and Manufacture 49 (2009) 832 – 842.

[34] L. Vela-Martínez, J. C. Jáuregui-Correa, E. Rodriguez, J. Álvarez Ramírez, Using detrended fluctuation analysis to monitor chattering in cutter tool machines, International Journal of Machine Tools and Manufacture 50 (2010) 651 – 657.

[35] E. Al-Regib, J. Ni, Chatter Detection in Machining Using Nonlinear Energy Operator, Journal of Dynamic Systems, Measurement, and Control 132 (2010) 034502.

[36] H. Caliskan, Z. Kilic, Y. Altintas, On-line energy-based milling chatter detection, ASME. J. Manuf. Sci. Eng. 140 (2018) 111012–1–111012–12.

[37] H. Cao, K. Zhou, X. Chen, X. Zhang, Early chatter detection in end milling based on multi-feature fusion and 3σ criterion, The International Journal of Advanced Manufacturing Technology 92 (2017) 4387–4397.

[38] R. Faassen, Chatter Prediction and Control for High-Speed Milling - Modelling and Experiments, Ph.D. thesis, Eindhoven University, 2007.

[39] N. J. M. van Dijk, E. J. J. Doppenberg, R. P. H. Faassen, N. van de Wouw, J. A. J. Oosterling, H. Nijmeijer, Automatic in-process chatter avoidance in the high-speed milling process, Journal of Dynamic Systems, Measurement, and Control 132 (2010) 031006–031006–14.

[40] A. Napolitano, Cyclostationarity: New trends and applications, Signal Processing 120 (2016) 385 – 408.

[41] A. Napolitano, Cyclostationarity: Limits and generalizations, Signal Processing 120 (2016) 323 – 347.

[42] J. Antoni, F. Bonnardot, A. Raad, M. E. Badaoui, Cyclostationary modelling of rotating machine vibration signals, Mechanical Systems and Signal Processing 18 (2004) 1285 – 1314.

[43] A. Raad, J. Antoni, M. Sidahmed, Indicators of cyclostationarity: Theory and application to gear fault monitoring, Mechanical Systems and Signal Processing 22 (2008) 574 – 587.

[44] M. Lamraoui, M. Thomas, M. E. Badaoui, F. Girardin, Indicators for monitoring chatter in milling based on instantaneous angular speeds, Mechanical Systems and Signal Processing 44 (2014) 72 – 85. Special Issue on Instantaneous Angular Speed (IAS) Processing and Angular Applications.

[45] M. Lamraoui, M. Thomas, M. E. Badaoui, Cyclostationarity approach for monitoring chatter and tool wear in high speed milling, Mechanical Systems and Signal Processing 44 (2014) 177 – 198. Special Issue on Instantaneous Angular Speed (IAS) Processing and Angular Applications.

[46] R. B. Randall, Vibration-based Condition Monitoring: Industrial, Aerospace and Automotive Applications, John Wiley and Sons, 2011.

[47] K. Fyfe, E. Munck, Analysis of computed order tracking, Mechanical Systems and Signal Processing 11 (1997) 187 – 205.

[48] P. Borghesani, R. Ricci, S. Chatterton, P. Pennacchi, A new procedure for using envelope analysis for rolling element bearing diagnostics in variable operating conditions, Mechanical Systems and Signal Processing 38 (2013) 23 – 35. Condition monitoring of machines in non-stationary operations.

[49] D. C. Montgomery, Introduction to statistical process control, John Wiley and Sons, 2009.

[50] Y. Altintas, Manufacturing Automation, Cambridge University Press, 2012.

[51] Y. Altintas, E. Budak, Analytical Prediction of Stability Lobes in Milling, CIRP Annals - Manufacturing Technology 44 (1995) 357–362.

[52] M. Zatarain, I. Bediaga, J. Munoa, R. Lizarralde, Stability of milling processes with continuous spindle speed variation: Analysis in the frequency and time domains, and experimental correlation, CIRP Annals 57 (2008) 379 – 384.